J. Bangladesh Acad. Sci. 49(1); 137-146 June 2025 DOI:https://doi.org/10.3329/jbas.v49i1.76826

Journal of Bangladesh Academy of Sciences

Journal homepage: http://www.bas.org.bd/publications/jbas.html

Research Article

Individual and combined effects of bicarbonate and calcium on phosphate adsorption to ferric (hydr)oxides

Rashedul Islam, Md Aktaruzzaman Sorid[1], Md Takibul Azad[1], Sumon Ganguli[2], Ashok Kumar Chakraborty[3], Mahbub Kabir[1] and Md Abdus Sabur[1*]

Department of Chemistry, Jashore University of Science and Technology, Jashore, Bangladesh

ARTICLE INFO

Article History

Received: 15 October 2024
Revised: 14 May 2025
Accepted: 15 May 2025

Keywords: Competitive effect, Adsorption, Desorption, Static and dynamic pH, Phosphate and ferric (hydr)oxides.

ABSTRACT

This study investigates how HCO_3^- and Ca^{2+} influence PO_4 adsorption onto ferric (hydr)oxide under static and dynamic pH conditions. Results show that HCO_3^- competes with PO_4 for surface binding sites, decreasing PO_4 adsorption under static pH conditions, while Ca^{2+} enhances PO_4 adsorption under alkaline conditions. At pH 8.0, 0.25 mM HCO_3^- reduces PO_4 adsorption, with a K_d value (the aqueous to solid-phase PO_4 ratio) 1.7 times higher than that observed in 10 mM NaCl. However, adding Ca^{2+} minimizes this effect of HCO_3^-, reducing K_d from 0.66 to 0.55, 0.37, and 0.24 with 0.05, 0.1, and 0.25 mM Ca^{2+}, respectively. Experiments under dynamic pH conditions show a similar trend, with K_d values approximately 84% lower than under static conditions, suggesting PO_4 immobilization on solid surfaces over time. These results indicate that elevated HCO_3^- concentrations may increase PO_4 mobility by reducing adsorption, while Ca^{2+} counteracts this effect under alkaline conditions.

Introduction

Phosphorus (P), in the form of phosphate ($H_nPO_4^{n-3}$, n=0, 1, 2, 3; hereafter PO_4), is an essential and often limiting nutrient for biological production (Smith and Schindler, 2009; Smolders et al., 2006). Phosphorus can be introduced to an aquatic environment from various points and nonpoint sources or can be released from bottom sediment into the overlying water column, a process known as internal P loading (Matisoff et al., 2016; Paytan et al., 2017; Smolders et al., 2006). This release typically occurs via mineral dissolution, desorption, and hydrolysis of organic P compounds (Joshi et al., 2015; Orihel et al., 2017). The solubility of both externally derived and sediment-released PO_4 in the water column is controlled by various biogeochemical factors, such as pH, redox potential, microbial activity, and the chemical composition of sediments and porewater (Filippelli, 2008; Ruttenberg, 2003; Sabur, 2019).

Naturally occurring anions such as bicarbonate (HCO_3^-), sulfate (SO_4^{2-}), and silicate (SiO_4^{4-}) may compete with PO_4 for the mineral binding sites, thereby increasing PO_4 concentrations in the aqueous phase (Antelo et al., 2007; Geelhoed et al., 1997; Sabur, 2019; Sabur et al., 2022; Smolders et al., 2006). Among these competitive anions, the HCO_3^- concentration is generally higher than PO_4 in natural waters (Sabur, 2019) and has been shown to promote PO_4 release from sediments (Smolders et al., 2006). However, in natural waters, particularly in systems buffered by carbonate minerals like calcite and

---

*Corresponding author:<sabur@juniv.edu>

[1] *Dept. of Chemistry, Jahangirnagar University, Dhaka, Bangladesh*

[2] *Biomaterials Research Laboratory, Dept. of Applied Chemistry and Chemical Engineering, University of Chittagong, Chittagong, Bangladesh;* [3] *Dept. of Applied Chemistry and Chemical Engineering, Islamic University, Khustia, Bangladesh*

dolomite—cations such as Ca^{2+} and Mg^{2+} are major chemical constituents alongside HCO_3^- (Langmuir, 1997b). Dissolved Ca^{2+} and Mg^{2+} have been shown to decrease the solubility of PO_4 in the aqueous phase through precipitation or co-precipitation as well as co-adsorption with PO_4 on mineral surfaces, particularly under alkaline conditions (Atouei et al., 2016; Rietra et al., 2001; Spiteri et al., 2008; Talebi et al., 2016).

While previous studies have explored the individual effects of bicarbonate and divalent cations (Ca^{2+}/ Mg^{2+}) on the mobility of PO_4 at the sediment-water interface, their combined effects of HCO_3^- and Ca^{2+} in regulating PO_4 mobility has not been comprehensively examined. The simultaneous effects of HCO_3^- and divalent cations such as Ca^{2+} and Mg^{2+} on PO_4 mobility at the sediment-water interface can be evaluated through experiments using natural sediments. While using natural sediments in experiments offers greater environmental realism, their inherently complex chemical and biological compositions can lead to numerous overlapping processes. Therefore, the HCO_3^- induced release of PO_4 from natural sediments, especially in the presence of divalent cations, may not fully capture the mechanisms by which HCO_3^- influences PO_4 mobility. These mechanisms can often be more effectively isolated by conducting experiments with clean minerals, such as ferric (hydr)oxides, rather than with natural sediments.

In this study, we examine the competitive effect of HCO_3^- on PO_4 adsorption onto ferric (hydr)oxide in both the absence and presence of dissolved Ca^{2+} across a range of static pH conditions. We also assess the effectiveness of HCO_3^- as a competing ion through PO_4 adsorption experiments conducted under static and dynamic pH conditions, with and without the presence of Ca^{2+}. Lastly, we compare the experimental results with water quality data from the US National Water Information Monitoring Database (NWIS) to identify aquatic environments that may experience HCO_3^- induced PO_4 mobility. We hypothesize that the cationic Ca^{2+} will counteract the anionic bicarbonate-induced PO_4 mobilization at the sediment-water interface.

Materials and Methods

Ferric (hydr)oxide synthesis

Ferric (hydr)oxide was synthesized by rapidly raising the pH of an acidic Fe^{3+} solution, following the method described by Schwertmann (1991). In brief, an acidic $FeCl_3$ solution was neutralized to pH 6.5 by the rapid addition of 1.0 M NaOH under continuous stirring at 100 rpm using an orbital shaker (Model: SO1). After 6 hours, the pH of the suspension dropped to 6.0 and was subsequently adjusted to pH 7.0 by adding 0.1 M NaOH. The resulting ferric (hydr)oxide precipitate was collected using a suction funnel, air-dried, and then oven-dried at approximately 105 °C. The dried material was ground with a mortar and pestle, sieved, and characterized using X-ray diffraction (XRD) and Fourier-transform infrared (FTIR) spectroscopy. The point of zero charge (PZC) of the synthesized ferric (hydr)oxides was determined to be 8.1 by potentiometric titration (Vakros et al., 2002). This dried and ground ferric (hydr)oxide was used in the PO_4 adsorption experiments.

Adsorption at static pH

First, a 0.25 mM phosphate (PO_4) solution (1.0 L) was prepared in 10 mM NaCl. This solution was divided into seven 100 mL aliquots, and the pH of each aliquot was independently adjusted within the range of 6.0 to 10.0 using dilute and concentrated HCl and NaOH. Next, 25 mL of each pH-adjusted PO_4 solution was added to a 50 mL polypropylene tube containing 0.0125 g of ferric (hydr)oxide (accurately weighed to four decimal places). The mixtures were shaken at 100 rpm on an orbital shaker (Model: SO1) for 2 hours to reach equilibrium, with pH adjustments made as needed during this period. Following equilibration, the suspensions were passed through a 0.45 µm syringe filter, and the phosphate concentrations in the filtrates were determined.

Additional pH-dependent PO_4 adsorption experiments were conducted using two other background solutions apart from 10 mM NaCl: (i) three $NaHCO_3$ solutions with concentrations of 0.25, 0.50, and 1.00 mM, and (ii) three $NaHCO_3$ (0.25 mM) solutions with varying Ca^{2+} concentrations of 0.05, 0.1, and 0.25 mM. The degree of PO_4 adsorption is expressed in the distribution constant (K_d), which represents the ratio of PO_4 in the aqueous phase to that in the solid phase. Lower K_d values indicate more effective removal of PO_4 from the aqueous phase, reflecting higher adsorption.

Adsorption at dynamic pH

Three sets of phosphate (PO_4) adsorption experiments were conducted under dynamic pH conditions. Set 1: Ferric (hydr)oxide (0.125 g) was equilibrated with 250 mL of a 0.25 mM PO_4 solution, prepared in 10 mM NaCl, for 4 hours. The pH of the suspension was initially adjusted to 5.0 using dilute and concentrated HCl and NaOH, creating a mildly acidic environment favorable for PO_4 adsorption. The pH was then adjusted to 6.0 and equilibrated for 4 hours, with periodic adjustments every 30 minutes to counter any drift. Following this, the pH was incrementally increased from 6.0 to 10.0 in one-unit intervals by adding NaOH. After 4 hours of equilibration at each pH level, samples were collected, filtered (0.45 µm pore size filter), and analyzed for aqueous PO_4 concentration. Set 2: To examine the effect of HCO_3^- on PO_4 adsorption, a 0.2275 mM PO_4 solution prepared in 10 mM NaCl and 225 mL was introduced into a reactor containing 0.125 g of ferric (hydr)oxide. Subsequently, 25 mL of a 2.5 mM $NaHCO_3$ solution was added, resulting in both PO_4 and HCO_3^- concentrations reaching 0.25 mM in the suspension, assuming no adsorption occurred. The pH was adjusted, and the suspension was equilibrated. Samples were then collected, filtered, and analyzed for PO_4 concentration following the same procedures as in Set 1. Set 3: The competitive effect of HCO_3^- on PO_4 adsorption was further evaluated in the presence of Ca^{2+}. Ferric (hydr)oxide (0.125 g) was equilibrated with 225 mL of a solution (225 mL) containing 0.2275 mM PO_4 and 0.28 mM Ca^{2+}, prepared in 10 mM NaCl. Then, 25 mL of a 2.5 mM $NaHCO_3$ solution was introduced to the system and equilibrated for 4 hours at pH 6. The procedures for adding HCO_3^-, adjusting the pH, and collecting and analyzing samples followed the same protocol described in Set 1.

Aqueous phosphate analysis

Phosphate concentrations in all experiments were determined spectrophotometrically by the molybdenum-blue method with maximum absorbance at 890 nm (Barman et al., 2024; Murphy and Riley, 1962; Nagul et al., 2015). For each set of experiments, the PO_4 concentrations were quantified by referencing them to a calibration curve constructed using a mixed matrix solution.

Results

Ferric (hydr)oxides characterization

The XRD pattern of the synthesized ferric (hydr)oxide (Fig. 1a) does not display distinctive features of mineral phases, suggesting that the product is primarily amorphous or poorly crystalline. However, a weak peak around ~35° 2θ may indicate the presence of ferrihydrite (Parmar and Parmar, 2020; Rani and Tiwari, 2017; Zhou et al., 2018). Fig. 1b and 1c show the FTIR spectroscopic data for the synthesized ferric (hydr)oxide, which exhibits several notable spectral bands. The peaks at 1489, 1339, and 446 cm^{-1} are characteristic spectral features of ferrihydrite (Liang et al., 2020). The 1628, 1070, 893, and 797 cm^{-1} peaks are associated with goethite (Liang et al., 2020; Liu et al., 2023). Additionally, FTIR features at 1628 and 1070 cm^{-1} may indicate hematite's presence, as supported by previous studies (Liu et al., 2023). Taken together with the XRD data, the FTIR spectra suggest that the synthesized ferric (hydr)oxide is predominantly amorphous. However, it may contain minor proportions of crystalline phases such as goethite and hematite.

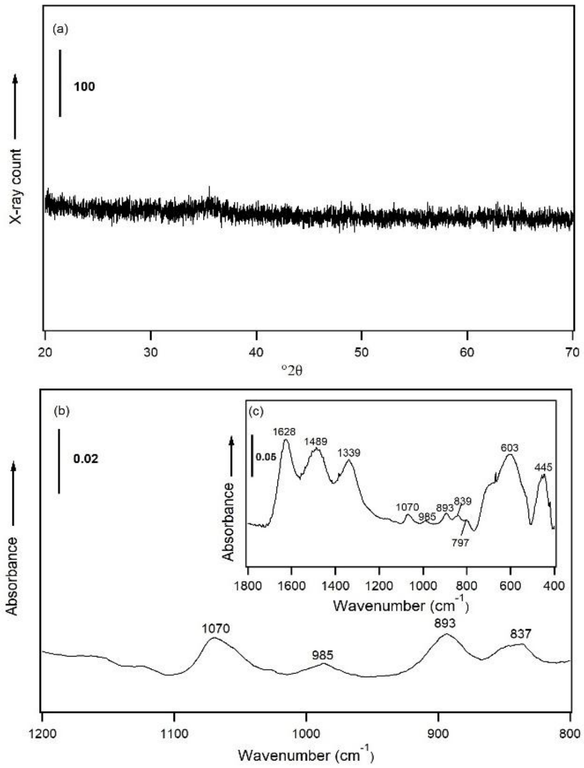

Fig. 1. XRD patterns (a) and FTIR spectra (b, c) of the dried ferric (hydr)oxide.

Adsorption at static pH

The adsorption of PO_4 onto ferric (hydr)oxides is influenced by the aqueous speciation of PO_4 and the protonation state of the solid surface (Gao and Mucci, 2001; Sabur et al., 2022; Spiteri et al., 2008). Generally, acidic pH conditions enhance PO_4 adsorption onto ferric (hydr)oxides compared to alkaline conditions (Li et al., 2016; Sabur et al., 2022). This is due to the increased hydroxyl ions (OH^-) concentration under alkaline conditions can create an unfavorable environment for PO_4 adsorption by acting as a competitive ions and increasing the surface's negative charge through OH^- adsorption (Li et al., 2016). Additionally, the chemical composition of the adsorption medium can affect PO_4 adsorption by altering its aqueous speciation and modifying the surface's electronic environment (Geelhoed et al., 1997; Sabur et al., 2022; Talebi et al., 2016). PO_4 can exist in several forms with different protonation states in aqueous solutions, such as H_3PO_4, $H_2PO_4^-$, HPO_4^{2-}, and PO_4^{3-}, depending on solution pH and chemical constituents (Li et al., 2016; Sabur et al., 2022). Consequently, speciation diagrams of PO_4 in different background solutions were generated (Fig. 2) using PHREEQC with the phreeqc.dat database (Parkhurst and Appelo, 2013).

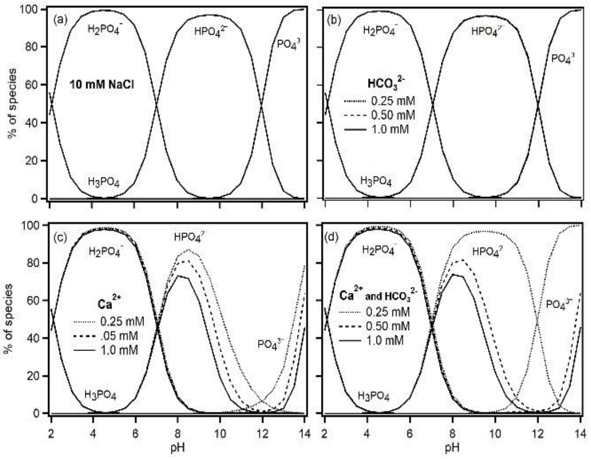

Fig. 2. Speciation of PO_4 (0.25 mM) in (a) NaCl (10 mM), (b) $NaHCO_3$ (0.25 to 1.0 mM) (c) $CaCl_2$ (0.25 to 1 mM), and (d) $CaCl_2$ and $NaHCO_3$ (0.25 to 1.0 mM Ca^{2+} and HCO_3^- ions) across a range of pH values at a temperature of 25 °C.

The phosphate adsorption experiments, both with and without HCO_3^-, reveal that HCO_3^- competes with PO_4 for surface binding sites on ferric (hydr)oxide, resulting in decreased PO_4 adsorption. This competitive effect becomes more pronounced with increasing HCO_3^- concentration, as expected (Fig. 3a). While the competitive effect HCO_3^- on PO_4 adsorption is minimal at or below pH 7.0, HCO_3^- significantly decreases PO_4 adsorption (i.e., K_d increases) as the pH increases from slightly alkaline to strongly alkaline conditions (Fig. 3a). For instance, at pH 8.0, the K_d values for PO_4 adsorption in the presence of three different HCO_3^- concentrations 1.7, 2.1, and 2.3 times higher than those in a 10 mM NaCl solution (0.39). At pH 10.0, these values increase to 3.4, 6.2, and 8.4 times compared to the value in NaCl solution (0.84).

Because with increasing pH, HCO_3^- gradually deprotonates and starts forming fully deprotonated CO_3^{2-} above pH 8.0 (Langmuir, 1997b) and effectively competes with PO_4 for the mineral binding sites (Gustafsson and Antelo, 2022; Mendez and Hiemstra, 2019; Rahnemaie et al., 2007).

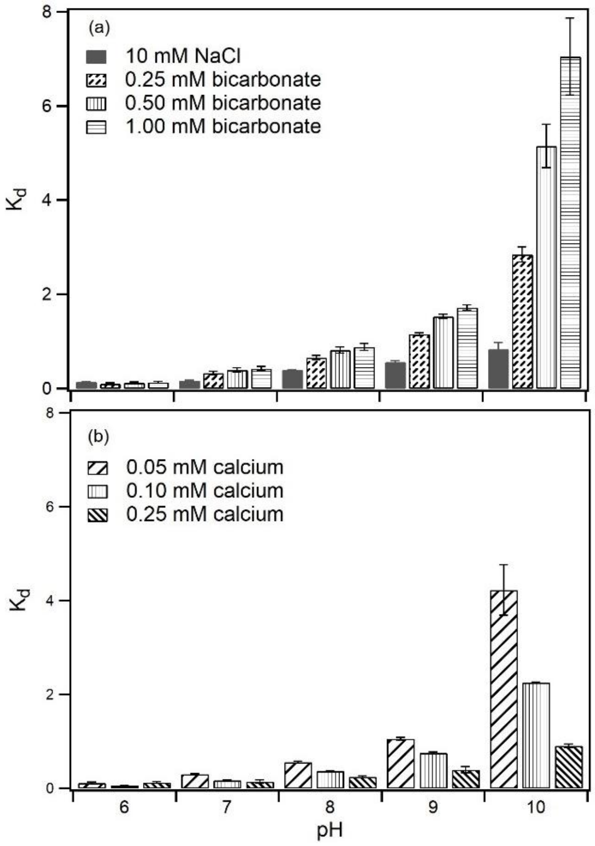

Fig. 3. PO_4 (0.25 mM) distribution constant (K_d) at the ferric (hydr)oxide-water interface in the presence of 0.25 to 1.0 mM HCO_3^- (a), and HCO_3^- (0.25 mM) plus Ca^{2+} concentrations (b) as a function of static pH at room temperature.

Divalent cations such as Ca^{2+} and Mg^{2+} are known to enhance PO_4 binding to ferric (hydr)oxides, particularly under alkaline pH conditions (Antelo et al., 2015; Atouei et al., 2016; Gustafsson and Antelo, 2022; Millero et al., 2001; Rietra et al., 2001). Generally, the adsorption of Ca^{2+} and Mg^{2+} ions to ferric (hydr)oxides increases with rising solution pH due to enhanced electrostatic attraction between the positively charged cations and the negatively charged surface (Spiteri et al., 2008; Talebi et al., 2016). In this study, PO_4 adsorption in HCO_3^- solution increases (i.e., the K_d value decreases) as both the concentration of Ca^{2+} and the pH rise (Fig. 3). The effect of Ca^{2+} on PO_4 adsorption becomes more pronounced with increasing Ca^{2+} concentrations. For example, at pH 8.0, the K_d value for PO_4 adsorption in the presence of 0.25 mM HCO_3^- is 0.66, which decreases to 0.55, 0.37, and 0.24 with the addition of 0.05, 0.1, and 0.25 mM Ca^{2+}, respectively. At pH 10.0, the K_d values for PO_4 adsorption in the presence of 0.25 mM HCO_3^- are 4.23, 2.26, and 0.90 with 0.05, 0.1, and 0.25 mM Ca^{2+}, respectively, compared to 2.85 in the presence of 0.25 mM HCO_3^- alone.

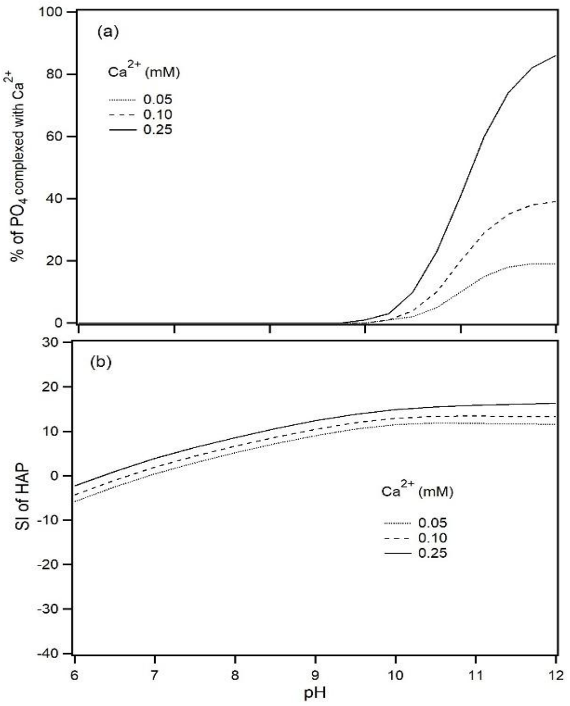

Fig. 4. (a) Percentage of total PO_4 (0.25 mM) complexed with calcium in the presence of 0.05, 0.1, and 0.25 mM Ca^{2+}. (b) Saturation indexes (SI) of hydroxyapatite under the given experimental conditions. The PO_4 speciation and SI values are computed using the PHREEQC Interactive 3.3.7 computer program and *phreeqc.dat* database (Parkhurst and Appelo, 2013), incorporating the dissociation constants of calcium phosphate

mineral phases (Dorozhkin, 2017; Shafii et al., 2024).

The higher K_d observed at pH 10.0 in the presence of both 0.25 mM HCO_3^- and 0.05 mM Ca^{2+}, compared to 0.25 mM HCO_3^- alone (Fig. 3), may be attributed to stronger aqueous complexation of PO_4 with Ca^{2+} (Fig. 4a), which reduces the affinity of PO_4 for the solid ferric (hydro)oxides, or to the precipitation or co-precipitation of PO_4 with Ca^{2+} on the solid surface.

The enhanced PO_4 adsorption with increasing (from 0.05 to 0.1 and 0.25 mM) Ca^{2+} concentrations can be attributed to the formation of calcium-phosphate (Ca-PO_4) phases (Islam et al., 2023), which is followed by the development of ternary surface complexes involving Ca^{2+} adsorbed onto the positively charged surface. Additionally, the removal of PO_4 from the solution via the formation of insoluble Ca-PO_4 complexes at higher Ca^{2+} concentrations is also thermodynamically feasible, as revealed from the calculated saturation index values (Fig. 4b), which increase with rising pH and Ca^{2+} concentrations (Ca/P ratios) (Antelo et al., 2015; Ler and Stanforth, 2003; Spiteri et al., 2008).

Adsorption at dynamic pH

The adsorption experiments were carried out using freshly synthesized ferric (hydr)oxide under controlled, constant pH conditions. In contrast, ferric (hydr)oxides in natural soils and sediments typically possess pre-adsorbed phosphate (PO_4) on their surfaces, and the pH in such environments tends to vary gradually over time. Therefore, we conducted PO_4 adsorption experiments under dynamic pH conditions, progressively adjusting the pH from 6.0 to 10.0. These dynamic pH envelope experiments were conducted in three different types of solution: (i) 10 mM NaCl, (ii) 0.25 mM HCO_3^-, and (iii) an equimolar concentration of HCO_3^- and Ca^{2+} ions (0.25 mM each). The results reveal that the K_d values for PO_4 adsorption under dynamic pH conditions decrease up to pH 8.0, followed by an increase (Fig. 5a), suggesting the release of adsorbed PO_4 occurs after pH 8.0 in the absence of HCO_3^-. Notably, in the presence of HCO_3^-, the K_d value increases with increasing pH, highlighting the competitive interaction of HCO_3^- with PO_4 for surface binding sites, also revealed in the static pH adsorption envelope experiments.

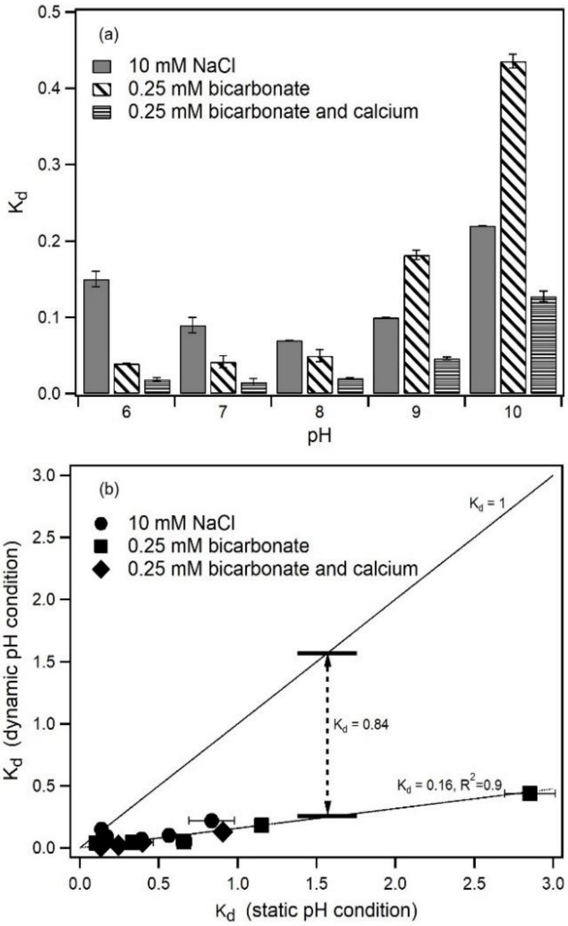

Fig. 5. PO_4 (0.25 mM) distribution constant (K_d) at the ferric (hydr)oxides-water interface under a dynamic pH condition (a). The comparison of K_d values under dynamic and static pH conditions (b).

When both HCO_3^- and Ca^{2+} are present, the K_d values remain relatively stable between pH 6.0 and 8.0 but increase above pH 8.0. Under alkaline conditions, the K_d values are generally higher in the HCO_3^- system than the NaCl system, with the lowest K_d values observed for the combined HCO_3^- and Ca^{2+} system (Fig. 5a), as expected. For example, at pH 9.0

and 10.0, the K_d values in the presence of 0.25 mM HCO_3^- increased to 0.18 and 0.44, respectively, compared to 0.10 and 0.22 in a 10 mM NaCl solution. In contrast, the K_d values for the equimolar concentrations of (0.25 mM) Ca^{2+} and HCO_3^- were 0.05 and 0.13 at pH 9.0 and 10.0, respectively.

The K_d values obtained under static and dynamic pH conditions are compared in Fig. 5b. The results indicate a significant difference between the two sets of K_d values. More specifically, the K_d values obtained from the PO_4 adsorption experiments conducted under dynamic pH conditions are considerably lower than those obtained under static pH conditions. For instance, the K_d (static) to K_d (dynamic) ratio is approximately 0.16, which is substantially less than the expected 1:1 ratio. This result suggests that PO_4 immobilization primarily occurs at the surface, with approximately 84% of the adsorbed-PO_4 remaining immobilized and not being released into the aqueous phase under dynamic pH conditions, in contrast to the observations made in the static pH condition experiments. This result implies that immobilization of PO_4 predominantly occurred on the surface (Ler and Stanforth, 2003; Sabur et al., 2022), possibly facilitated by the formation of stronger binding interactions with surface functional groups. This binding mechanism could hinder the release of adsorbed PO_4 into the aqueous phase. For example, adsorbed-PO_4 may gradually form stronger complexes with ferric iron present on the solid surface (Ler and Stanforth, 2003) or may form stable surface complexes (e.g., bi-dentate) via the transformation of weaker (e.g., outer-sphere and/or mono-dentate) complexes during the pH transition from acidic to alkaline conditions (Sabur et al., 2022; Zhong et al., 2007).

Discussion and significance

Bicarbonate tends to form surface complexes with ferric (hydr)oxide that are less stable than those formed with PO_4, as demonstrated in previous research (Rahnemaie et al., 2007). However, the HCO_3^- concentrations in natural waters are typically higher than PO_4 (Sabur, 2019). Generally, HCO_3 in natural waters is regulated by several factors, including the diffusion of CO_2 from the atmosphere, the dissolution of carbonate minerals (e.g., calcite, aragonite, and dolomite), as well as fluvial input (Langmuir, 1997b). Additionally, the relative rates of photosynthesis and respiration often play a role in controlling HCO_3^- concentrations in surface waters (Langmuir, 1997b; Verspagen et al., 2014). For instance, dissolved CO_2 and HCO_3^- are consumed by primary producers during photosynthesis, with HCO_3^- being generated as a byproduct of organic matter mineralization (Verspagen et al., 2014).

Calcium ions enter aquatic environments through fluvial transport, groundwater flow, and the dissolution of carbonate minerals like calcite and dolomite (Cerar and Urbanc, 2013; Langmuir, 1997a). The dissolution of typical carbonate minerals results in an aqueous phase molar ratio of Ca^{2+} to HCO_3^-/CO_3^{2-} at ~1:1 (Cerar and Urbanc, 2013). However, data from the US National Water Information System (NWIS) indicate that the concentration of HCO_3^- in natural waters is approximately ten times higher than that of Ca^{2+} (Fig. 6). The surface water HCO_3^- and Ca^{2+} concentrations (ponds, impoundments, and lakes) indicate the contribution of other sources (e.g., organic matter mineralization) involved for in-situ generation of HCO_3^- (Langmuir, 1997b). The NWIS data were extracted from the US NWIS database using the USGS parameter codes 00453 and 0915, respectively. The concentrations of HCO_3^- and Ca^{2+} were extracted (between 2010 and 2016) for common sampling stations and dates of sampling from all water depths available in the database.

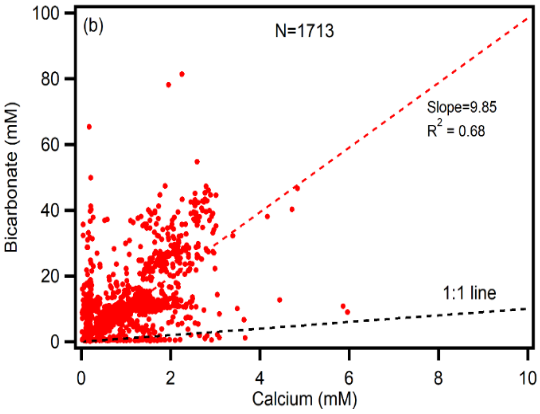

Fig. 6. Concentrations of HCO_3^- with respect to Ca^{2+} in surface waters (ponds, impoundments, and lakes) according to the US NWIS database (2010 - 2016).

Elevated PO_4 concentrations in natural waters often correlate with HCO_3^- (Smolders et al., 2006), indicating that HCO_3^- may slightly enhance PO_4 mobility by reducing its adsorption. However, the release of phosphate (PO_4^{3-}) from mineral surfaces induced by bicarbonate (HCO_3^-) is unlikely, particularly in the presence of naturally occurring cations such as calcium (Ca^{2+}). Nevertheless, in aquatic environments where HCO_3^- primarily arises from the mineralization of organic carbon rather than the dissolution of carbonate minerals, HCO_3^- may contribute to enhanced PO_4 mobility.

Conclusions

In this study, we examine the individual and combined effects of HCO_3^- and Ca^{2+} ions on the mobility of phosphate (PO_4) at the ferric (hydr)oxide–water interface under both static and dynamic pH conditions. Our adsorption pH envelope experiments demonstrate that HCO_3^- can compete with PO_4 for binding sites on mineral surfaces. However, in the presence of Ca^{2+}, this competitive effect is diminished, particularly under alkaline pH conditions.

Results from adsorption experiments under dynamic pH conditions further show that the ability of HCO_3^- to act as a desorbing agent for PO_4 is relatively weak, especially when Ca^{2+} is also present. In natural waters, where HCO_3^- concentrations are significantly higher than those of PO_4^{3-}, HCO_3^- may enhance the mobility of PO_4 by reducing its adsorption to mineral surfaces. Nonetheless, in aquatic systems buffered by carbonate mineral dissolution, the coexistence of Ca^{2+} can mitigate the competitive influence of HCO_3^-, thereby limiting the mobility of dissolved phosphate.

Acknowledgment

The authors are thankful to the University Grants Commission of Bangladesh for financial support.

Disclosure statement

The authors do not have any conflict of interest regarding the publication of this manuscript.

References

Antelo J, Arce F and Fiol S. Arsenate and phosphate adsorption on ferrihydrite nanoparticles. *Chem. Geol.* 2015; 410: 53-62.

Antelo J, Arce F, Avena M, Fiol S, López R and Macías F. Adsorption of a soil humic acid at the surface of goethite and its competitive interaction with phosphate. *Geoderma,* 2007; 138(1-2): 12-19.

Atouei MT, Rahnemaie R, Kalanpa EG and Davoodi MH. Competitive adsorption of magnesium and calcium with phosphate at the goethite water interface: Kinetics, equilibrium and CD-MUSIC modeling. *Chem. Geol.* 2016; 437(25): 19-29.

Barman DK, Islam R, Dash GK, Ganguli S, Chakraborty AK, Kabir M and Sabur MA. Interfering effect of silicate in the quantification of phosphate by the molybdenum-blue method. *Asian J. Water Environ. Pollut.* 2024: 21(6): 195-20.

Cerar S and Urbanc J. Carbonate chemistry and isotope characteristics of groundwater of Ljubljansko Polje and Ljubljansko Barje aquifers in Slovenia. *Sci. World J.* 2013.

Dorozhkin SV. Calcium orthophosphates (CaPO4): occurrence and properties. *Prog. Biomater.* 2017; 5(1): 9-70.

Filippelli GM. The global phosphorus cycle: past, present, and future. *Elements*, 2008; 4(2): 89-95.

Gao Y and Mucci A. Acid base reactions, phosphate and arsenate complexation, and their competitive adsorption at the surface of goethite in 0.7 M NaCl solution. *Geoch. Cosmochim. Acta,* 2001; 65(14): 2361-2378.

Geelhoed JS, Hiemstra T and Van Riemsdijk WH. Phosphate and sulfate adsorption on goethite: single anion and competitive adsorption. *Geoch. Cosmochim. Acta,* 1997; 61(12): 2389-2396.

Gustafsson JP and Antelo J. Competitive arsenate and phosphate adsorption on ferrihydrite as described by the CD-MUSIC model. *ACS Earth*

Space Chem. 2022; 6(5): 1397-1406.

Islam R, Barman DK, Kabir M and Sabur MA. Salinity-induced phosphate binding to soil particles: Effects of divalent cations. *Water Air Soil Pollut.* 2023; 234(11): 697.

Joshi SR, Kukkadapu RK, Burdige DJ, Bowden ME, Sparks DL and Jaisi DP. Organic matter remineralization predominates phosphorus cycling in the mid-bay sediments in the Chesapeake Bay. *Environ. Sci. Technol.* 2015; 49(10): 5887-5896.

Langmuir D. *Aqueous Environmental Geochemistry.* McConnin R., ed., 1st ed., Prentice-Hall. Inc. 1997a. p. 618.

Langmuir D. Carbonate chemistry. In: *Aqueous Environmental Geochemistry.* McConnin R., ed., Prentice-Hall. Inc. 1997b; pp. 193-230.

Ler A and Stanforth R. Evidence for surface precipitation of phosphate on goethite. *Environ. Sci. Technol.* 2003; 37(12): 2694-2700.

Li M, Liu J, Xu Y and Qian G. Phosphate adsorption on metal oxides and metal hydroxides: A comparative review. *Environ. Rev.* 2016; 24(3): 319-332.

Liang C, Tang B, Zhang X and Fu F. Mobility and transformation of Cr (VI) on the surface of goethite in the presence of oxalic acid and Mn (II). *Environ. Sci. Pollut. Res.* 2020; 27: 26115-26124.

Liu R, Kong S, Shao Y, Cai D, Bai B, Wei X and Chorover J. Mechanisms and health implications of toxicity increment from arsenate-containing iron minerals through in vitro gastrointestinal digestion. *Geoderma*, 2023; 432: 116377.

Matisoff G, Kaltenberg EM, Steely RL, Hummel SK, Seo J, Gibbons KJ, Bridgeman TB, Seo Y, Behbahani M, James WF, Johnson LT, Doan P, Dittrich M, Anne M and Chaf JD. Internal loading of phosphorus in western Lake Erie. *J. Great Lakes Res.* 2016; 42(4): 775-788.

Mendez JC and Hiemstra T. Carbonate adsorption to ferrihydrite: Competitive interaction with phosphate for use in soil systems. *ACS Earth Space Chem.* 2019: 3(1): 129-141.

Millero F, Huang F, Zhu X, Liu X and Zhang JZ. Adsorption and desorption of phosphate on calcite and aragonite in seawater. *Aquat. Geochem.* 2001: 7(1): 33-56.

Murphy J and Riley JP. A modified single solution method for the determination of phosphate in natural waters. *Anal. Chim. Acta*, 1962; 27: 31-36.

Nagul EA, McKelvie ID, Worsfold P and Kolev SD. The molybdenum blue reaction for the determination of orthophosphate revisited: opening the black box. *Anal. Chim. Acta*, 2015; 890: 60-82.

Orihel DM, Baulch HM, Casson NJ, North RL, Parsons CT, Seckar DCM and Venkiteswaran JJ. Internal phosphorus loading in Canadian fresh waters: a critical review and data analysis. *Can. J. Fish. Aquat. Sci.* 2017; 74(12): 2005-2029.

Parkhurst DL and Appelo CAJ. Description of input and examples for PHREEQC version 3:A computer program for speciation, batch-reaction, one-dimensional transport, and inverse geochemical calculations. In: *Techniques and Methods.* U.S. Geological Survey, USA, 2013.

Parmar C and Parmar GS. Structural and magnetic properties of six-line ferrihydrite nanoparticles. *J. Supercond. Nov. Magn.* 2020; 33: 441-444.

Paytan A, Roberts K, Watson S, Peek S, Chuang P, Defforey D and Kendall C. Internal loading of phosphate in Lake Erie Central Basin. *Sci. Total Environ.* 2017; 579: 1356-1365.

Rahnemaie R, Hiemstra T and van Riemsdijk WH. Carbonate adsorption on goethite in competition with phosphate. *J. Colloid Interface Sci.* 2007; 315(2): 415-425.

Rani C and Tiwari SD. Phase transitions in two-line ferrihydrite nanoparticles. *Appl. Phys. A*, 2017; 123; 1-4.

Rietra RPJJ, Hiemstra T and Van Riemsdijk WH. Interaction between calcium and phosphate adsorption on goethite. *Environ. Sci. Technol.* 2001; 35(16): 3369-3374.

Ruttenberg KC. The global phosphorus cycle. In: *Treatise on Geochemistry,* Turekian KK, Holland HD, eds., 1st ed., 2003; pp. 585-643.

Sabur MA. *Interactions of Phosphate and Silicate with Iron oxides in Freshwater Environments*. Ph.D. Theis, University of Waterloo, Ontario, Canada, 2019.

Sabur MA, Parsons CT, Maavara T and Van Cappellen P. Effects of pH and dissolved silicate on phosphate mineral-water partitioning with goethite. *ACS Earth Space Chem*. 2022; 6(1): 34-43.

Schwertmann U. Solubility and dissolution of iron oxides. *Plant Soil*, 1991; 130(1-2): 1-25.

Shafii M, Slowinski S, Sabur MA, Arvisais A, Bhusal Y, Withers W, Krogstad JK, Parsons CT and Van Cappellen P. Mineral formation explains the high retention efficiency of dissolved reactive phosphorus in a residential stormwater pond. *Env. Sci.: Adv.* 2024; 3(6): 819-832.

Smith VH and Schindler DW. Eutrophication science: where do we go from here? *Trends Ecol. Evol.* 2009; 24(4): 201-207.

Smolders AJP, Lamers LPM, Lucassen ECHET, van Der Velde G and Roelofs JGM. Internal eutrophication: how it works and what to do about it – a review. *Chem. Ecol.* 2006; 22(2): 93-111.

Spiteri C, Cappellen P Van and Regnier P. Surface complexation effects on phosphate adsorption to ferric iron oxyhydroxides along pH and salinity gradients in estuaries and coastal aquifers. Geochim. Cosmochin. Acta, 2008; 72(14): 3431-3445.

Talebi M, Rahnemaie R, Goli E and Hossein M. Competitive adsorption of magnesium and calcium with phosphate at the goethite water interface: kinetics, equilibrium and CD-MUSIC modeling. *Chem. Geol.* 2016; 437: 19-29.

Vakros J, Kordulis C and Lycourghiotis A. Potentiometric mass titrations: a quick scan for determining the point of zero charge. *Chem. Commun.* 2002; 17: 1980-1981.

Verspagen JMH, Van de Waal DB, Finke JF, Visser PM, Van Donk E and Huisman J. Rising CO2 levels will intensify phytoplankton blooms in eutrophic and hypertrophiclakes. *PloS One*, 2014; 9(8): e104325.

Zhong B, Stanforth R, Wu S and Chen JP. Proton interaction in phosphate adsorption onto goethite. *J. Colloid Interface Sci.* 2007; 308(1): 40-48.

Zhou S, Sato T and Otake, T. Dissolved silica effects on adsorption and co-precipitation of Sb (III) and Sb (V) with ferrihydrite. *Minerals*, 2018; 8(3): 101.